AIAA JOURNAL
Vol. 34, No. 2, February 1996

Semiactive Vibration Suppression by Variable-Damping Members

Junjiro Onoda* and Kenji Minesugi†
Institute for Space and Astronautical Science, Sagamihara, Kanagawa 229, Japan

A semiactive vibration suppression approach is proposed and investigated. It is to control the damping of viscous dampers installed in structures. By using a single-degree-of-freedom (SDOF) example first, vibration damping is shown to be much enhanced by a suitable variation of the damping of the damper according to the phase of vibration. Next, several types of control logic for this approach are proposed, which are applicable to multiple-degree-of-freedom (MDOF) structures with multiple variable dampers. The performance of these types of control logic are investigated by using an SDOF example and an MDOF truss structure example with three variable-damping truss members excited by impulsive and random forces. Numerical investigations demonstrate that the vibration suppression capabilities of most of them are much higher than that of the optimally tuned passive system, keeping the robustness of passive systems.

I. Introduction

TO suppress the vibration of space structures, active vibration suppression is very attractive and powerful.[1] Numerous works have been published on the subject, with various types of actuators. Although many works have been published on robust control logic, the technology is still experiencing problems with instability due to phenomena such as spillover.[2] On the other hand, passive systems, which have no artificial controls and whose vibration energy is dissipated by the structural damping, viscosity, friction, etc., are always stable. This robustness is their great advantage. In many cases, however, passive systems have disadvantages in their damping performance. A possible attractive approach to reduce this disadvantage, keeping the advantages of passive systems, may be semiactive vibration suppression, which controls the states of systems such that their inherent damping performances are enhanced.

With a semiactive approach, vibration is suppressed by passive energy dissipation mechanisms. Therefore, systems are always stable even when the control logic is improper due to lack of exact information about the dynamic characteristic of the structures. In the case of space structures that are deployed or constructed in orbit, exact estimation of the dynamic characteristics is very difficult. In addition, very high reliability is required for the space structural systems. Therefore, the robust semiactive approaches seem to be suitable for space structures.

Several types of semiactive vibration suppression have been proposed and studied. For space truss structures, Onoda et al.[3] proposed and investigated a vibration suppression by stiffness control using a hysteretic variable-stiffness member that is called type-II in their paper. They also proposed to control the friction for semiactive vibration suppression of truss structures[4] and tension-stabilized structures.[5] To suppress the vibration of a mechanical system, Karnopp et al.[6] proposed to vary the damping of a dashpot type damper. This type of semiactive approach has been studied mainly for ground vehicles[7,8] and buildings.[9,10] In these studies, the variable-damping dampers are directly connected to lumped masses. To apply the approach to flexible space structures, it may be better to study based on more suitable mathematical model, which may require other control logic.

In this paper, a semiactive vibration suppression is proposed and investigated, which is to control the damping of dashpot-type passive dampers in the structures. By using a single-degree-of-freedom (SDOF) system example that simulates a flexible system, it is first shown that the vibration damping can be much enhanced by varying the damping of the damper according to the phase of vibration. Next, several types of control logic are proposed, which are practically applicable to multiple-degree-of-freedom (MDOF) structures with multiple variable dampers. The performances of these control laws are investigated and compared with each other by using an SDOF system example and an MDOF truss beam example. Numerical simulations demonstrate that most of them are much more effective than optimally tuned passive dampers for the truss structure excited by impulsive and random forces.

Some may be concerned about the practicality of the application of dashpot-type variable dampers in space, which contain fluid. However, D-strut[11] is an example that seems to be applicable to the space structures. Variable-damping dampers may be a combination of this type of damper and a variable-area orifice. Electrorheological (ER) fluid may be used instead of the variable-area orifice.

II. Vibration Suppression Enhancement by a Variable-Damping Element

Let us first investigate the SDOF system shown in Fig. 1. The system between the mass and the base in the figure is a simplified model of a dashpot-type damper.[11] Because of spring k_2, this system is different from those studied in Refs. 6–9, which model vibration isolator. Without k_2, the system does not vibrate when c is large, which is not the actual situation of flexible structures. Therefore the system shown in Fig. 1 represents the flexible structures with a damper more suitably. If we vary the orifice area of D-strut[11] by an electromagnetic valve, c can be varied independently from the equivalent stiffness of the damper model.

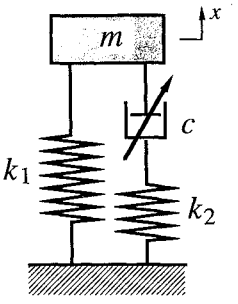

Fig. 1 Single-degree-of-freedom system with variable-damping element.

Presented as Paper 94-1770 at the AIAA/ASME Adaptive Structures Forum, Hilton Head, SC, April 21–22, 1994; received June 13, 1994; revision received Aug. 14, 1995; accepted for publication Aug. 20, 1995.

*Professor, Research Division for Space Transportation. Member AIAA.
†Associate Professor, Research Division for Space Transportation. Member AIAA.

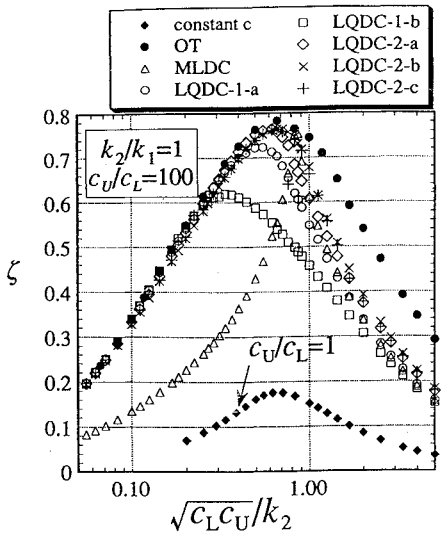

Fig. 2 Damping rates of SDOF system from various control laws (k_2/k_1 = 1.0).

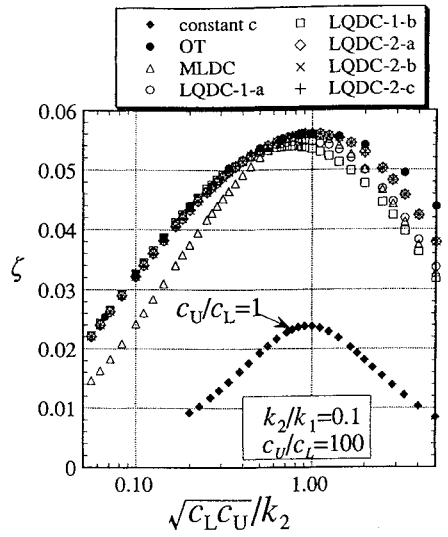

Fig. 3 Damping rates of SDOF system from various control laws (k_2/k_1 = 0.1).

When the external force is absent, the equations of motion of this system are

$$m\ddot{x} + k_1 x + k_2(x - e) = 0 \tag{1}$$

$$\dot{e} = (x - e)k_2/c \tag{2}$$

where x is the displacement of the mass, e is the elongation of the dashpot element, and c is its damping that is variable in the range

$$c_L \le c \le c_U \tag{3}$$

In this paper, we define the effective damping rate as

$$\zeta = -\ell n(a_{n+1}/a_n)/[T\sqrt{(k_1 + k_2)/m}] \tag{4}$$

where a_n is the amplitude of the nth cycle, and T is the duration of a cycle. Because the cycle duration is a function of c, which will be varied in the subsequent section, we use ζ defined as in Eq. (4), which represents the damping per time rather than per cycle.

When $c_L = c_U$, i.e., when c is constant, the effective damping rates can be numerically calculated as a function of $\sqrt{(c_U c_L)}/k_2$ as plotted in Figs. 2 and 3 noted as constant c, respectively. Figure 2 is the case of $k_2/k_1 = 1.0$, whereas $k_2/k_1 = 0.1$ in Fig. 3.

Next, to investigate if a higher damping rate is available by varying the damping c according to the phase of vibration, let us assume that

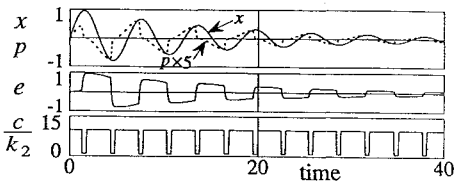

Fig. 4 Example of time history of the response of SDOF system controlled by OT control law [k_2/k_1 = 0.1 and $\sqrt{(c_U c_L)}/k_2$ = 1.0].

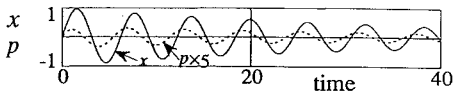

Fig. 5 Example of time history of the response of optimally tuned passive SDOF system (k_2/k_1 = 0.1 and $c_U/k_2 = c_L/k_2$ = 1).

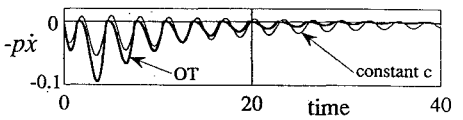

Fig. 6 Energy supply rate from the damper.

the value of c_U is much larger than c_L, and let us minimize c when

$$(x + \varphi_1\dot{x})(\dot{x} - \varphi_2 x) < 0 \tag{5}$$

holds, and keep c maximum during the rest of the cycle, where φ_1 and φ_2 are constants representing the timings of the reduction and recovery of c. The control logic of Eq. (5) is suggested from the study on variable-stiffness systems,[3] which is identical with the present system when $c_L = 0$ and c_U is infinitely large. Furthermore, let us optimize the values of φ_1 and φ_2 such that the vibration damping rate is maximized. Then, the damping rates are obtained as functions of $\sqrt{(c_U c_L)}/k_2$ as plotted in Figs. 2 and 3 noted as optimal timing (OT). In these examples, c_U/c_L is fixed to 100 as an example. These values of damping rate are obtained from numerically simulated time histories of free decay vibrations after enough number of cycles.

The figures show that the damping rate largely depends on the value of k_2/k_1 in both constant c and OT cases. However, regardless of the value of k_2/k_1, a much higher damping rate has been obtained by varying c with optimal timing than that of passive system. Roughly maximum damping rate is obtained when $\varphi_1 = 7.0$, $\varphi_2 = 1.8$, and $\sqrt{(c_U c_L)}/k_2 = \frac{2}{3}$ in Fig. 2, and when $\varphi_1 = 4.0$, $\varphi_2 = 0.26$, and $\sqrt{(c_U c_L)}/k_2 = 1$ in Fig. 3. The optimal timings of the reduction and recovery (i.e., φ_1 and φ_2) are functions of $\sqrt{(c_U c_L)}/k_2$ and c_U/c_L. But it may not be straightforward to obtain the functions explicitly. Furthermore, the extension of this control logic to MDOF systems with multiple variable-damping elements does not seem to be easy. Therefore, it is necessary to find more convenient approaches.

Figures 4 and 5 show time histories of the SDOF system whose k_2/k_1 is 0.1, where p is the load on the damper. Figure 4 is the case of semiactive control by OT law with the optimal value of $\sqrt{(c_U c_L)}/k_2$, which give the maximum ζ in the OT plots in Fig. 3. Figure 5 shows the time histories of an optimal passive system, whose value of c/k_2 gives the maximum ζ in the constant c plots in Fig. 3. In Fig. 4, the values of e and p vary stepwise according to the control of c, whereas p varies sinusoidally in Fig. 5. Figure 6 shows the time history of $-p\dot{x}$ of the two cases shown in Figs. 4 and 5, which is the work done by the damper to the mass. As shown in the figure, the work done by the damper is never positive in the case of a semiactively controlled system, indicating that the damper always removes the energy from the mass. However, in the case of a passive system, it is positive for short periods. Furthermore, because of the larger amplitude of stepwise varying p of Fig. 4, the negative work done by the controlled damper is larger than that of the passive damper in the initial phase. These reasons are why the vibration damping can be enhanced by the control of c.

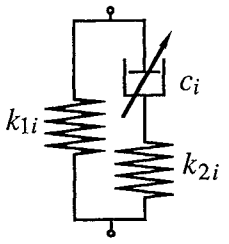

Fig. 7 Mathematical model of ith variable-damping truss member.

III. Equations of Motion of MDOF Systems with Variable-Damping Elements

To investigate the control logic that is applicable to MDOF systems with multiple variable-damping elements, let us first derive their equations of motion. As an example of an MDOF system with multiple variable-damping elements, let us investigate a truss structure that has n_a variable-damping members whose axial characteristics can be modeled as in Fig. 7. When the external force is absent and the structural damping is negligible, the equations of motion of this system are written in the physical coordinate as

$$M\ddot{x} + Kx + HDe = 0 \tag{6}$$

$$\dot{e} = -CD(H^T x + e) \tag{7}$$

where

$$D = \text{diag}[k_{2i}] \tag{8}$$

$$C = \text{diag}[1/c_i] \tag{9}$$

$$e = \lfloor e_1, e_2, \ldots, e_{n_a} \rfloor \tag{10}$$

and x is the displacement vector, M is the mass matrix, K is the stiffness matrix that includes both k_{1i} and k_{2i} of all of the variable-damping members, H is a matrix composed of directional cosines of variable-damping truss members, k_{1i} and k_{2i} are the spring constants shown in Fig. 4, c_i is the value of c, and e_i is the elongation of the dashpot element of the ith active member, respectively.

In the modal coordinate, the equations of motion are written as

$$\ddot{q} + \Omega q + \Phi^T HDe = 0 \tag{11}$$

$$\dot{e} = -CD(H^T \Phi q + e) \tag{12}$$

where

$$\Omega = \text{diag}\left(\omega_1^2, \ldots, \omega_m^2\right) \tag{13}$$

$$\Phi = (\phi_1, \ldots, \phi_m) \tag{14}$$

and q is the displacement vector in the modal coordinates, and ω_i and ϕ_i are the angular frequency and mode shape of the ith mode obtained from M and K matrices of Eq. (6) (i.e., those of the structure whose values of c are all infinitely large). In this paper, the value of c_i is assumed to be limited in the range

$$c_{Li} \le c_i \le c_{Ui} \tag{15}$$

IV. Control Strategies for Variable-Damping Structures

Maximum Load Damping Control (MLDC)

When the values of c_{Li} are small and those of c_{Ui} are large enough, the present system becomes similar to the type-II variable-stiffness system investigated in Ref. 3. Therefore, from the analogy with control logic C of the reference, the following on-off control law seems to be effective: 1) minimize c_i when $|p_i|$ is at a maximum, 2) maximize c_i when p_i becomes zero or when $|p_i|$ starts to increase before reaching zero; where p_i is the load transferred through the ith variable damper. The time history of Fig. 4 qualitatively supports this control law. This control law is simple and can be easily applied to the MDOF systems with multiple variable-damping elements. In addition, it is suitable for distributed control because only the locally available information is required for the control of each variable damper. In this paper, this control law is referred to as MLDC.

Linear Quadratic Damping Control-1 (LQDC-1)

Equation (11) can be rewritten as

$$\dot{z}_1 = A_1 z_1 + B_1 e \tag{16}$$

where

$$z_1 = \lfloor q^T, \dot{q}^T \rfloor^T \tag{17}$$

$$A_1 = \begin{bmatrix} 0 & I \\ -\Omega & 0 \end{bmatrix} \tag{18}$$

$$B_1 = \begin{bmatrix} 0 \\ -\Phi^T HD \end{bmatrix} \tag{19}$$

and I is a unit matrix. Equation (16) shows that we could apply the well-developed linear control theories if we could directly control e of this system. As the linear quadratic regulator (LQR) control theory, it is known[12] that the optimal linear control that minimizes

$$J \equiv \int_0^\infty \left(z_1^T R_1 z_1 + e^T R_2 e\right) \mathrm{d}t \tag{20}$$

is to control e as

$$e = e_T \equiv -F_1 z_1 \tag{21}$$

where R_1 and R_2 are weighting matrices, F_1 is a gain matrix given by

$$F_1 = R_2^{-1} B_1^T P_1 \tag{22}$$

and P_1 is the positive-definite solution of the following Riccati equation:

$$P_1 B_1^T R_2^{-1} B_1 P_1 - A_1^T P_1 - P_1 A_1 - R_1 = 0 \tag{23}$$

In the present system, we cannot directly control e. However, the preceding investigation suggests that a promising approach for vibration suppression of the present system is to control c_i such that e traces e_T defined by Eq. (21) as exactly as possible. Since a lower value of c_i promotes the variation of e_i as shown in Eqs. (7) and (9), a possible strategy is to reduce c_i as long as e_i is varying toward e_{Ti} to promote the variation. Otherwise, it is to maximize c_i to keep e_i close to e_{Ti}, where e_{Ti} is the ith element of e_T. This strategy can be implemented by the following control law:

$$\begin{aligned} c_i &= c_{Li} \quad \text{when} \quad \dot{e}_i(e_{Ti} - e_i) > 0 \\ c_i &= c_{Ui} \quad \text{when} \quad \dot{e}_i(e_{Ti} - e_i) < 0 \end{aligned} \tag{24}$$

In this paper, this control law is called as LQDC-1-a.

In the LQR control, a large value of e results in a large penalty as shown by the term that includes R_1 in Eq. (20). However, in the present system, a large value of e does not necessarily require large energy, and it is not necessary to penalize it. Therefore, better performance may be obtained by controlling c_i such that the absolute value of e_i becomes maximum when the sign of e_i is the same as that of e_{Ti}, and otherwise such that it becomes minimum. This strategy can be implemented by the following control law:

$$\begin{aligned} c_i &= c_{Li} \quad \text{when} \quad \dot{e}_i e_{Ti} > 0 \\ c_i &= c_{Ui} \quad \text{when} \quad \dot{e}_i e_{Ti} < 0 \end{aligned} \tag{25}$$

We can see that this control law promotes the variation of e_i when e_i is moving towards the polarity of e_{Ti}, and otherwise depress its motion. In this paper, this control law is called as LQDC-1-b.

Linear Quadratic Damping Control-2 (LQDC-2)

Equations (11) and (12) can be combined and rewritten as

$$\dot{z}_2 = A_2 z_2 + B_2 v \tag{26}$$

where

$$z_2 = \lfloor q^T, \dot{q}^T, e^T \rfloor^T \tag{27}$$

$$A_2 = \begin{bmatrix} 0 & I & 0 \\ -\Omega & 0 & \Phi^T H D \\ 0 & 0 & 0 \end{bmatrix} \tag{28}$$

$$B_2 = \begin{bmatrix} 0 \\ 0 \\ I \end{bmatrix} \tag{29}$$

$$v = -CD(H^T \Phi q + e) \tag{30}$$

If we could control the value of v without any limitation, the LQR control logic tells us that v should be controlled such that

$$v = v_T \equiv -F_2 z_2 \tag{31}$$

where F_2 is the gain matrix given by the LQR control theory similarly as Eqs. (22) and (23).

In the present case, as shown by Eqs. (9) and (30), the ith element of v, v_i, is inversely proportional to c_i, which can be directly controlled. However, the value of c_i is limited in the range of Eq. (15). Therefore, as with LQDC-1, a possible strategy is to control the value of c_i such that the value of v_i becomes as close to v_{Ti} as possible, where v_{Ti} is the ith element of vector v. This strategy can be implemented by

$$\begin{aligned} c_i &= p_i/v_{Ti} \quad \text{when} \quad c_{Li} < p_i/v_{Ti} < c_{Ui} \\ c_i &= c_{Li} \quad \text{when} \quad p_i/v_{Ti} < c_{Li} \\ c_i &= c_{Ui} \quad \text{when} \quad c_{Ui} < p_i/v_{Ti} \end{aligned} \tag{32}$$

where p_i is the ith element of p defined as

$$p = -D(H^T \Phi q + e) \tag{33}$$

In this paper, this control law is called as LQDC-2-c.

To apply LQDC-2-c, the damping c_i of each variable damping members has to be continuously variable. Such a continuously variable damping member may be heavier, more complex, and more expensive than an on-off type variable-damping member whose c_i is either c_{Li} or c_{Ui}. A control strategy for the systems with such on-off type variable-damping members is to select the value of c_i that gives closer value of v_i to v_{Ti} than the other value does. This strategy can be implemented by

$$\begin{aligned} c_i &= c_{Ui} \quad \text{when} \quad (v_{Ti} - v_{Ai})(v_{Ui} - v_{Ai}) > 0 \\ c_i &= c_{Li} \quad \text{when} \quad (v_{Ti} - v_{Ai})(v_{Ui} - v_{Ai}) < 0 \end{aligned} \tag{34}$$

where

$$\begin{aligned} v_{Li} &= p_i/c_{Li} \\ v_{Ui} &= p_i/c_{Ui} \end{aligned} \tag{35}$$

and v_{Ai} is an average of v_{Ui} and v_{Li}. This control law is called LQDC-2-a in this paper.

As with LQDC-1, a large value of v_i does not cost in the present system. Therefore, another possible approach is to make the absolute value of v_i maximum when the polarities of v_i and v_{Ti} are identical, and otherwise to make the absolute value of v_i minimum. This strategy can be implemented by the following control law:

$$\begin{aligned} c_i &= c_{Li} \quad \text{when} \quad v_i v_{Ti} > 0 \\ c_i &= c_{Ui} \quad \text{when} \quad v_i v_{Ti} < 0 \end{aligned} \tag{36}$$

This control law is called as LDQC-2-b in this paper.

V. Numerical Examples of an SDOF System

MLDC, LQDC-1, and LQDC-2 control laws are applied to the SDOF system shown in Fig. 1. The value of c_U/c_L is assumed to be 100. In LQDC-1 and LQDC-2, all of the elements of R_1 are set to be zero except for $R_1(1, 1)$ and $R_1(2, 2)$, where $R_1(i, j)$ is the ith row jth column element of matrix R_1. The term $R_1(1, 1)$ is set as $(k_1 + k_2)/m$, and the values of $R_1(2, 2)$ and R_2 are roughly optimized by trial and error so that the value of ζ becomes maximum. These values are shown in Table 1. In LQDC-2-c, the geometrical mean is used for v_{Ai} of Eq. (34) because it gives better results in this example than the arithmetic mean. Figures 2 and 3 show the resulting damping rates from these control laws as functions of $\sqrt{(c_U c_L)}/k_2$, which are obtained by numerical simulations.

The figures show that these control laws result in a much higher damping rate than that of optimally tuned constant c, demonstrating their effectiveness. When $k_2/k_1 = 1$, the performance of MLDC is excellent only when the value of $\sqrt{(c_U c_L)}/k_2$ is optimal as shown in Fig. 2. The performances of LQDC-2 control laws are also excellent. Furthermore, they are relatively insensitive to the variation of $\sqrt{(c_U c_L)}/k_2$. At the optimal value of $\sqrt{(c_U c_L)}/k_2$, the performances of LQDC-2 control laws are almost the same as that of OT, which is the maximum damping rate achieved by a cycle of on-off variation of c per half-cycle of vibration. The performances of LQDC-1 are also relatively insensitive to the variation of $\sqrt{(c_U c_L)}/k_2$, although the damping rates are slightly less than those of LQDC-2 control laws.

When $k_2/k_1 = 0.1$ also, the damping rates are substantially increased by the control of c as shown in Fig. 3, although the damping rates are lower than those of Fig. 2 in all of the cases. In this case, the differences in the performances of the control laws are relatively small, although the damping rates from LQDC-1 control laws are slightly lower than those from the others. Unlike the previous case, the performance of MLDC is relatively insensitive to the variation of $\sqrt{(c_U c_L)}/k_2$ in this case.

VI. Numerical Examples of MDOF System

To investigate the effectiveness of the aforementioned vibration suppression control laws in MDOF systems with multiple variable-damping elements, we studied vibration suppression of a truss shown in Fig. 8. The truss has three variable-damping members, which are modeled as Fig. 7. The axial stiffness EA of each passive member is unity. The mass per unit length of each member is unity including the variable-damping members. The length of the members l is also unity except for the diagonal members. In this examples, k_{1i} and k_{2i} (shown in Fig. 7) are assumed to be

$$k_{1i} = k_{2i} = EA/(2l_i) \qquad i = 1, 2, 3 \tag{37}$$

Table 1 Roughly optimal parameter values used for numerical investigation of SDOF system

	$k_2/k_1 = 1$		$k_2/k_1 = 0.1$	
	$R_1(2, 2)$	$R_2/2$	$R_1(2, 2)$	$R_2/2$
LQDC-1-a	5×10^2	$2k_1/m$	1×10^3	$5k_1/m$
LQDC-1-b	1×10^3	$1 \times 10^3 k_1/m$	1	$1 \times 10^6 k_1/m$
LQDC-2-a	1×10^3	1×10^{-2}	1×10^5	2×10^{-3}
LQDC-2-b	1×10^3	2×10^{-2}	1×10^5	2×10^{-3}
LQDC-2-c	5×10^2	1×10^{-2}	1×10^5	2×10^{-3}

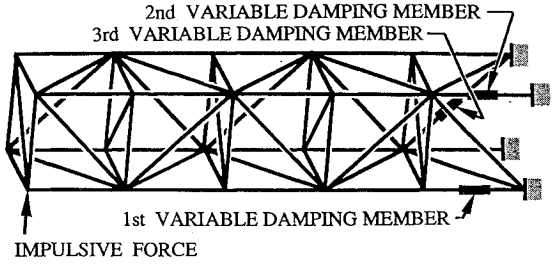

Fig. 8 Truss structure with variable-damping truss members.

where l_i is the length of the ith variable-damping member. Furthermore, it is also assumed that

$$c_{Ui}/c_{Li} = 100 \qquad i = 1, 2, 3 \tag{38}$$

and the values of $\sqrt{(c_U c_L)}/k_2$ of variable-damping members are identical with each other as

$$\sqrt{c_{Ui}c_{Li}}/k_{2i} = \sqrt{c_U c_L}/k_2 \qquad i = 1, 2, 3 \tag{39}$$

A unit impulsive load is applied as shown in Fig. 8, and the subsequent vibration suppression by each control law is numerically simulated. In the simulation, all of the 60 modes are included in the mathematical model without any modal truncation. To measure the performance of each control law, the value of

$$I_1 = \int_0^{16\pi/\omega_1} \delta_{\mathrm{rms}}\, \mathrm{d}t \tag{40}$$

is calculated, where δ_{rms} is the root-mean-square (rms) displacement of the truss nodes. In LQDC-1 control laws, matrix R_1 is set as

$$R_1 = \mathrm{diag}\left(1, 1, \ldots, 1, r_1/\omega_1^2, r_1/\omega_2^2, \ldots, r_1/\omega_{n_c}^2\right) \tag{41}$$

and it is set as

$$R_1 = \mathrm{diag}\left(1, 1, \ldots, 1, r_1/\omega_1^2, r_1/\omega_2^2, \ldots, r_1/\omega_{n_c}^2, 0\right) \tag{42}$$

for LQDC-2 control laws, where r_1 is a constant, and n_c is the number of controlled modes. In both LQDC-1 and 2 control laws, the lowest five modes are controlled (i.e., $n_c = 5$), and R_2 is set as

$$R_2 = r_2 I \tag{43}$$

for both LQDC-1 and 2 control laws, where r_2 is a constant. The values of r_1 and r_2 are roughly optimized by trial and error so that the value of I_1 becomes minimum. The roughly optimal values, which are used for the following simulation examples, are listed in Table 2.

The values of I_1 obtained by numerical simulations by using the various control laws are plotted in Fig. 9 as functions of $\sqrt{(c_U c_L)}/k_2$. The values of I_1 of passive system, whose various c are constant (i.e., $c_{Ui} = c_{Li}$), are also plotted. In this case also, the values of $\sqrt{(c_U c_L)}/k_2$ of the damping members are assumed to be identical with each other as Eq. (39).

Figure 9 shows that all of the control laws are effective in comparison with the passive (i.e., constant c) system except for MLDC. Unlike the previous case of SDOF system, MLDC is not very effective. This is because of excessively frequent variation of c resulting from the high-frequency component in the load signal, which MLDC control law monitors. The values of I_1 noted as MLDC-5 in the figure are also obtained from an MLDC control law. However, in this case, the value of c is controlled based on the load caused by the lowest five modes instead of the actual load. By using the lower modes component only, the excessive variation of c has been remedied, and the damping performance has been increased. However, this control law requires the modal data, which are not necessary for the original MLDC control law.

When the value of $\sqrt{(c_U c_L)}/k_2$ is optimal, Fig. 9 shows that LQDC-1-a is the best, and LQDC-2-b is the second in their performance. Generally, the sensitivities of the performance of the semiactive approaches to the relative variation of $\sqrt{(c_U c_L)}/k_2$ are less than that of the passive system. Especially, the performance of LQDC-2-c is excellent in most wide range of $\sqrt{(c_U c_L)}/k_2$. The best values of I_1 of each control law in Fig. 9 are listed in Table 3 in comparison with the value of I_1 of the structure whose modal damping is 0.5%. The table indicates that the value of I_1 has been substantially reduced by the vibration suppression approaches, especially by the semiactive approaches other than MLDC.

Figure 10 shows an example of time history of the response of the truss with LQDC-1-a control law with optimal value of $\sqrt{(c_U c_L)}/k_2$. The figure shows that the vibration, especially the lower mode vibration, is suppressed nicely. We can see that the values of the various e trace their target values e_T (which are shown by broken lines) when it is possible. However, e_i can be increased or decreased only when the load on the damper is tensile or compressive, respectively. The values of c_1 and c_3 are reduced mainly at the peaks of $|q_3|$ and $|q_1|$, respectively, as in Fig. 4. However, c_2 looks to respond various modes. The time history of δ_{rms} suggests that the higher mode variations, which are not shown in the figure, are not so large as to significantly contribute to δ_{rms} at $t\omega_1 = 50$.

Table 2 Roughly optimal parameter values used for numerical investigation of MDOF system

	r_1	r_2
LQDC-1-a	100	10
LQDC-1-b	0.1	1×10^4
LQDC-2-a	0.1	100
LQDC-2-b	0.5	5
LQDC-2-c	1	100

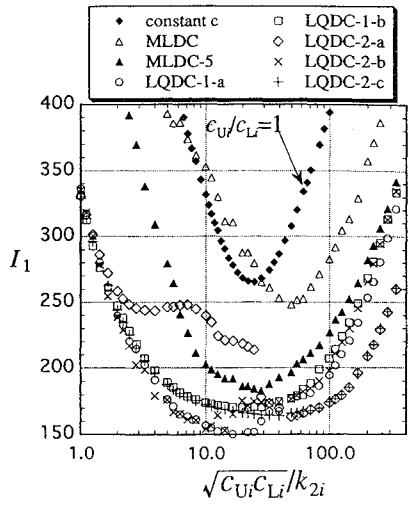

Fig. 9 Values of I_1 resulting from various control laws applied to a truss structure.

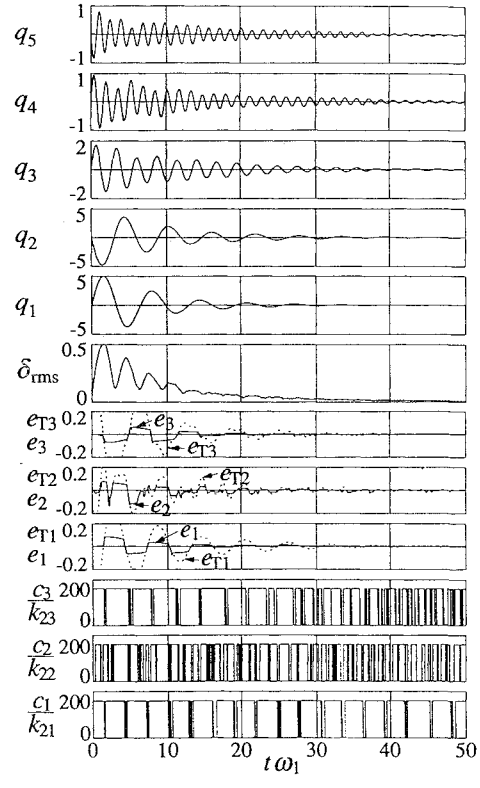

Fig. 10 Example of time history of vibration suppression by LQDC-1-a control law (impulsive excitation).

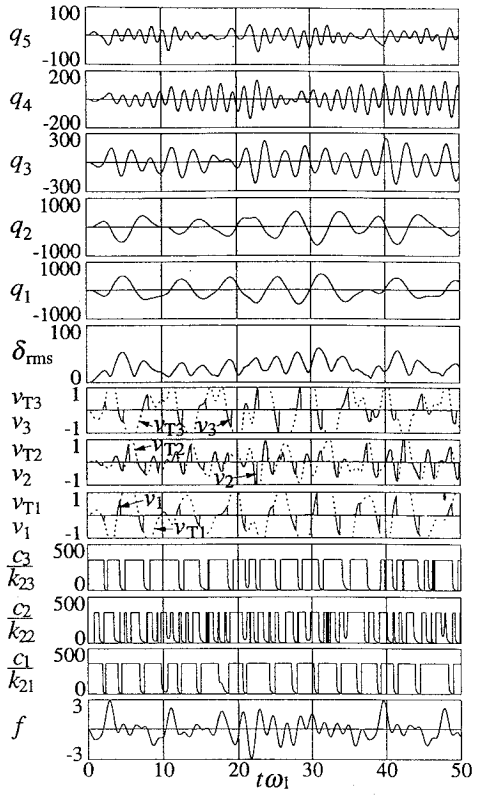

Fig. 11 Example of time history of vibration suppression by LQDC-2-c control law (random excitation).

Next, random force is applied to the truss structure, and the aforementioned semiactive and passive approaches are applied to reduce the response of the truss. The direction and the attach point of the random force are the same as those of the impulsive force shown in Fig. 8. As shown in Fig. 11 denoted as f, a random force time history is generated and applied to the simulation, whose rms value is unity. The power spectral density (PSD) per unit angular frequency of the random force is flat in the range from $0.7\omega_1$ to $4.1\omega_1$ and zero in the other frequency range. This frequency range of nonzero PSD covers ω_1–ω_4. The parameter values shown in Table 2, which are roughly optimal for the impulsive excitation, are used for these numerical simulations. To measure the performances of the control laws, the value of

$$I_2 = \int_{8\pi/\omega_1}^{16\pi/\omega_1} \delta_{rms}\, dt \tag{44}$$

is calculated. The values of I_2 obtained from various control laws are plotted in Fig. 12 as functions of $\sqrt{(c_U c_L)}/k_2$. The value of I_2 of a passive system is also plotted. In Fig. 12, the performance of LQDC-1-a is again the best. The differences between the minimum values from MLDC-5, LQDC-1-b, and LQDC-2 control laws are smaller than those of Fig. 9. The value of $\sqrt{(c_U c_L)}/k_2$ that gives the best performance of MLDC is slightly lower than that of Fig. 9. However, we can see that Fig. 12 is similar to Fig. 9. This fact suggests that the semiactive control investigated here is effective for the random excitation similarly as the impulsive excitation.

Figure 11 shows an example of time history of the truss structure that is controlled by LQDC-2-c. The values of v trace their target values v_T only when it is possible. As shown in the figure, the values of c are varied continuously unlike Fig. 10. As with Fig. 10, c_1 and c_3 are decreased mainly at the peaks of $|q_3|$ and $|q_1|$, respectively.

The best values of I_2 of each control law in Fig. 12 are listed in Table 3. In the case of random force excitation also, the value of I_2 has been substantially reduced by the passive and semiactive approaches compared with the case of 0.5% modal damping. We can see that the control law that gives smaller value of I_1 for impulsive excitation gives a smaller value of I_2 for the random excitation also, demonstrating its effectiveness for the random excitation. It is

Table 3 Minimum values of I_1 and I_2 from various approaches

	I_1	I_2	I_1/I_2	$\sqrt{I_1}/I_2$
0.5% damping	645.6	64,348	0.0100	$3.95E$-4
Constant c	265.1	36,916	0.00718	$4.41E$-4
MLDC	248.1	32,361	0.00766	$4.87E$-4
MLDC-5	182.9	27,716	0.00660	$4.88E$-4
LQDC-1-a	149.8	26,209	0.00572	$4.67E$-4
LQDC-1-b	170.3	27,503	0.00619	$4.74E$-4
LQDC-2-a	167.9	27,503	0.00610	$4.71E$-4
LQDC-2-b	153.2	27,947	0.00548	$4.43E$-4
LQDC-2-c	164.1	27,368	0.00600	$4.68E$-4

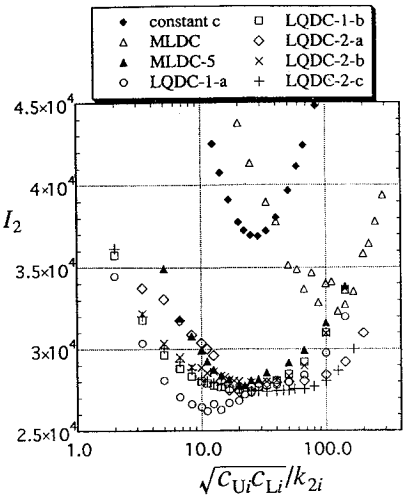

Fig. 12 Value of I_2 resulting from various control laws applied to a truss structure.

reasonable that the value of I_2 obtained from each control law is roughly proportional to $\sqrt{I_1}$ rather than I_1.

VII. Concluding Remarks

A semiactive vibration suppression has been proposed and studied. The approach is to control the damping of dampers installed in structures. Several control laws are proposed, which are applicable to MDOF structures with multiple variable dampers. To study the performance of these control laws, numerical simulations have been performed by using an SDOF example and an MDOF truss example. The numerical simulation results have demonstrated that all of them result in substantially higher vibration damping rate than that of the optimally tuned passive system in the case of SDOF system. In the case of an MDOF truss with multiple variable damper also, the results have demonstrated that all of these control laws except for one reduce the response of the structure to the impulsive and random excitation to a substantially lower level than that of optimally tuned passive system, demonstrating their effectiveness.

With semiactive vibration suppression, the energy is dissipated by passive mechanisms. Therefore, unlike with the active vibration suppression, the system is always stable even when the control system is improperly designed. Furthermore, the performance of semiactive vibration suppression is much higher than passive vibration suppression. Therefore, semiactive vibration suppression is an attractive approach for space structures that will be deployed or constructed in the orbit, whose control system design is difficult because of the lack of exact information about its dynamic characteristics. However, to apply this approach to actual space structure, much more study is required.

References

[1]Balas, M. J., "Trends in Large Space Structure Control Theory: Fondest Hopes, Wildest Dreams," *IEEE Transactions on Automatic Control*, Vol. AC-27, No. 3, 1982, pp. 522–535.

[2]Balas, M. J., "Active Control of Flexible Systems," *Journal of Optimization Theory and Applications*, Vol. 25, No. 3, 1978, pp. 415–436.

[3]Onoda, J., Endo, T., Tamaoki, H., and Watanabe, N., "Vibration Suppression by Variable-Stiffness Members," *AIAA Journal*, Vol. 29, No. 6, 1991, pp. 977–983.

[4]Onoda, J., and Minesugi, K., "Semi-Active Vibration Suppression of Truss Structures by Coulomb Friction," *Journal of Spacecraft and Rockets*, Vol. 31, No. 1, 1994, pp. 67–74.

[5]Onoda, J., Sano, T., and Kamiyama, K., "Active, Passive and Semi-Active Vibration Suppression by Stiffness Variation," *AIAA Journal*, Vol. 30, No. 12, 1992, pp. 2922–2929.

[6]Karnopp, D., Crosby, M. J., and Harwood, R. A., "Vibration Control Using Semi-Active Force Generator," *Journal of Engineering for Industry*, Vol. 96, May 1974, pp. 619–626.

[7]Rakheja, S., and Sankar, S., "Vibration and Shock Isolation Performance of a Semi-Active 'On-Off' Damper," *Journal of Vibration, Acoustics, Stress, and Reliability in Design*, Vol. 107, Oct. 1985, pp. 398–403.

[8]Hrovat, D., Margolis, D. L., and Hubbard, M., "An Approach Toward the Optimal Semi-Active Suspension," *Journal of Dynamic Systems, Measurement, and Control*, Vol. 110, Sept. 1988, pp. 288–296.

[9]Kobori, T., Takahashi, M., Niwa, N., and Kurata, N., "Research on Active Seismic Response Control System with Variable Structure Characteristics—Feedback Control with Variable Stiffness and Damping Mechanism," *Journal of Structural Engineering of Architectural Institute of Japan*, Vol. 37B, March 1991, pp. 193–202 (in Japanese).

[10]Kobori, T., Takahashi, M., Nasu, T., Niwa, N., Ogasawara, K., Kurata, N., and Mizuno, T., "Research on Active Seismic Response Control System with Variable Structure Characteristics—Basic Property of Variable Stiffness and Damping Mechanism and Fundamental Experiment by Shaking Table," *Journal of Structural Engineering of Architectural Institute of Japan*, Vol. 37B, March 1991, pp. 183–291 (in Japanese).

[11]Davis, L. P., Workman, B. J., Chu, C. C., and Anderson, E. H., "Design of a D-Strut and Its Application Results in the JPL, MIT and LARC Test Bed," *Proceedings of the AIAA/ASME/ASCE/AHS/ASC 33rd Structures, Structural Dynamics, and Materials Conference* (Dallas, TX), AIAA, Washington, DC, 1992, pp. 1524–1530 (AIAA Paper 92-2274).

[12]Kwakernaak, H., and Sivan, R., *Linear Optimal Control System*, Wiley-Interscience, New York, 1972.